

Adaptive Local-Global Relational Network for Facial Action Units Recognition and Facial Paralysis Estimation

Xuri Ge, Joemon M. Jose, Pengcheng Wang, Arunachalam Iyer, Xiao Liu, and Hu Han, *Member, IEEE*

Abstract— Facial action units (AUs) refer to a unique set of facial muscle movements at certain facial locations defined by the Facial Action Coding System (FACS), which can be used for describing nearly any anatomically possible facial expression. Many existing facial action units (AUs) recognition approaches often enhance the AU representation by combining local features from multiple independent branches, each corresponding to a different AU, which usually neglect potential mutual assistance and exclusion relationship between AU branches or simply employ a pre-defined and fixed knowledge-graph as a prior. In addition, extracting features from pre-defined AU regions of regular shapes limits the representation ability. In this paper, we propose a novel Adaptive Local-Global Relational Network (ALGRNet) for facial AU recognition and apply it to facial paralysis estimation. ALGRNet mainly consists of three novel structures, *i.e.*, an adaptive region learning module which learns the adaptive muscle regions based on the detected landmarks, a skip-BiLSTM module which models the latent mutual assistance and exclusion relationship among local AU features, and a feature fusion&refining module which explores the complementarity between local AUs and the whole face for the local AU refinement. In order to evaluate our proposed method, we migrated ALGRNet to a facial paralysis dataset which is collected and annotated by medical professionals. Experiments on the BP4D and DISFA AU datasets show that the proposed approach outperforms the state-of-the-art methods by a large margin. Additionally, we also demonstrated the effectiveness of the proposed ALGRNet in applications to facial paralysis estimation.

Index Terms— Facial action units, Facial paralysis estimation, Skip-BiLSTM, Fusion&Refining, Multi-branch

We thank Professor Brian O'reilly for sharing part of the facial paralysis dataset.

Xuri Ge is with the School of Computing Science, University of Glasgow, Scotland, UK (e-mail: x.ge.2@research.gla.ac.uk).

Joemon M. Jose is with the School of Computing Science, University of Glasgow, Scotland, UK (e-mail: joemon.jose@glasgow.ac.uk).

Pengcheng Wang is with Tomorrow Advancing Life Education Group (TAL), Beijing 100080, China (e-mail: wangpengcheng2@tal.com).

Arunachalam Iyer is with the Department of Otolaryngology and Head and Neck Surgery, University Hospital Monklands, Airdrie, Scotland, UK, and also with University of Glasgow, Scotland, UK (aruniyerent@gmail.com).

Xiao Liu is with the Online Media Business Unit at Tencent, Beijing 100080, China (e-mail: ender.liux@gmail.com).

Hu Han is with the Key Laboratory of Intelligent Information Processing, Institute of Computing Technology, Chinese Academy of Sciences, Beijing 100190, China, and also with Peng Cheng Laboratory, Shenzhen 518055, China (e-mail: hanhu@ict.ac.cn).

I. INTRODUCTION

RECENTLY, facial action units recognition has attracted increasing research attention in computer vision due to its wide range of potential applications in facial state analysis, *i.e.*, diagnosing mental disease [1], improving e-learning experiences [2], deception detection [3], face recognition and attribute estimation [4], assisting teaching in education [5], *etc.* However, in the literature it is rare to see such studies that extending the AU recognition model to the assessment of facial paralysis grades. Facial Palsy is the temporary or permanent weakness or lack of movement affecting one side of the face and is an acute, unilateral facial nerve weakness or paralysis of rapid onset (less than 72 hours) and unknown cause. It affects around 23 per 100,000 people per year, and current methods to estimate the severity is subjective process. In fact, the severity of facial paralysis can be estimated by the manifestations of several muscle areas of the face together, which is really similar to the representation of individual expressions using the Facial Action Coding System (FACS) [6]. In this study, we propose a novel AU recognition model and explore its ability to estimate facial paralysis severity.

AU recognition is challenging due to the difficulty of recognizing subtle facial changes caused by AUs. Looking from biological perspective, the activation of AU corresponds to the movement of facial muscles, which inspired earlier works such as [7], [8] to design hand-crafted features to represent the appearance of different local facial regions. However, hand-crafted features are not discriminative enough to represent the facial morphology due to their shallow natures. Hence, deep learning based methods for AU recognition have been investigated in recent years to enhance the feature representation of AUs.

Many existing automatic facial AU recognition methods aim to enhance the facial feature representation by combining local features from multiple independent branches, which are related to different AU regions. Some grid-based deep learning frameworks [9], [10] incorporate regional (patch-based) Convolutional Neural Network (CNN) features from a face with equal grids, as shown in Fig. 1 (a). For instance, the scheme in [11] combines local CNN features from equal partition grids by an LSTM [12]. However, dividing images into fixed grids leads to a number of issues: (i) it is difficult to focus exactly on the muscle area corresponding to each AU; (ii) ROIs for AUs with irregular shapes may

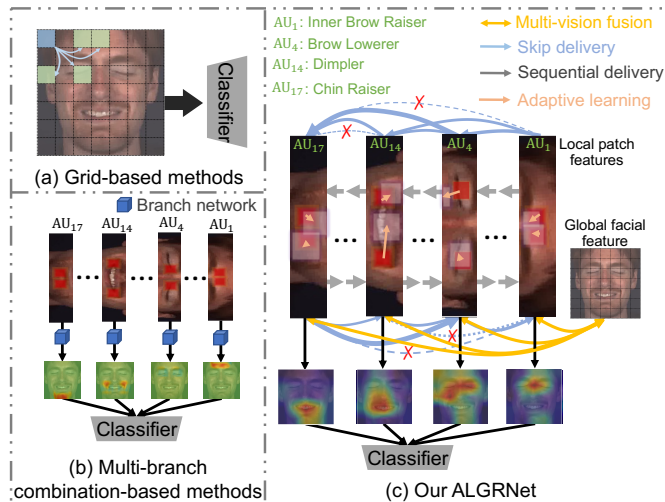


Fig. 1. Illustration of the different AU feature learning and classification schemes: (a) the traditional grid-based feature extraction and classification, (b) the multi-branch combination-based recognition methods, and (c) our ALGRNet method. Compared with (a) and (b), our ALGRNet adaptively adjusts the AU areas in terms of different individuals based on detected landmarks, exploits mutual assistance and mutual exclusion relations of local facial patch-based multiple branches via a novel bi-directional structure with skipping gates and refines their irregular representations by the global facial feature (best viewed in color).

not be well represented by grid-based features. To address the above issues, recent popular multi-branch combination-based methods [13]–[15] fuse global or local features from independent AU branches based on the corresponding muscle region detection, to refine the features for AUs with irregular regions, as shown in Fig. 1 (b). For instance, an end-to-end multi-branch framework in [16] is proposed to joint AU detection and face alignment, which combines the features from independent branches for individual AU related muscle regions according to some predefined attention maps based on detected landmarks. Moreover, the latest approach [15] propose a local AU recognition loss to refine the local attention maps by close area pixel contributions for each AU in the independent branches instead of the predefined attention maps, which also neglects mutual relationships among the multiple branches for each face. While the multi-branch combination based AU recognition methods show their effectiveness in local AU feature fusion, there are still limitations in modeling mutual relationship among adaptive AU regions as well as modelling the local and global context. Firstly, unlike the localisation of corresponding AU regions based on fixed landmarks, adaptive learning of AU regions (shape and position) can improve the robustness of the model based on the diversity of expressions and individual characteristics, which however is usually neglected by the exiting literature. Secondly, the multiple patches related to individual AUs, may have a strong positive or negative latent correlation in most expressions. Here, if multiple AUs jointly affect the target AU category, it is defined as positive correlation (mutual assistance), otherwise negative correlation (mutual exclusion). For example, adjacent AU2 (“Outer Brow Raiser”) and AU7 (“Lid Tightener”) will be activated simultaneously when scaring, and non-adjacent

AU6 (“Cheek Raiser”) and AU12 (“Lip Corner Puller”) will be activated simultaneously when smiling. Inspired by these biological phenomena, we argue that capturing the interactive information relationship between patch-based branches, such as sequential/skipping delivery of adjacent/non-adjacent related regions, is important for enhancing the representation of AU features. Finally, the global face feature provides important cues to refine the limited regular patch features, which is important to deal with irregular muscle shapes. This is because the local AU patches may not cover the entire face, and other non-AU regions may also be activated due to muscle linkage.

To address the above problems, we propose a novel ALGRNet for facial AU recognition and apply it on facial paralysis estimation task. In particular, we first extract the grid-based global feature by multi-layer CNNs and local AU features based on the detected facial landmarks. Different from previous methods, we adapt to different individuals and expressions by learning from landmark offsets. We then design a skip-BiLSTM to capture the potential assistance and exclusion relations among these sequential branches, where the adjacent patches are adjustable transfer in BiLSTM [17] while the distant patches are connected via skipping-type gates. We argue that each AU branch is independent and equal, so such a skip connection manner can minimize the loss of information compared with traditional BiLSTM. Moreover, we design a novel feature fusion&refining module to refine the local features from skip-BiLSTM guided by global grid-based features. Different with previous feature fusion methods [15], our gated fusion architecture in feature fusion&refining module can appropriately supplement global information, even non-AU region information, for each local AU patches. It is very important because different AUs may focus on different global information. Finally, the features learned by ALGRNet are fed to a multi-branch classification network for AU recognition.

The contributions of our ALGRNet for facial AU recognition are as follows:

- We propose a skip-BiLSTM approach to model the mutual assistance and exclusion relationship of individual AUs based on the learned adaptive landmarks, which leads to improved robustness in AU recognition;
- We propose a method for local AU feature refinement with the assistant of global grid-based features, making the local AU features more discriminative;
- The proposed ALGRNet outperforms the state-of-the-art approaches for AU recognition on two benchmarks, *i.e.*, BP4D and DISFA, without any external data or pre-trained models in additional data. Moreover, we collect a facial paralysis dataset, named FPar, to verify that the proposed AU recognition model can be applied to facial paralysis estimation and achieves superior performance than the baseline methods.

In comparison to the earlier conference version [18] of this work, we propose a new adaptive region learning module in Section III-B in order to further improve the accuracy of muscle regions and to better adapt to irregular muscle

shapes. In particular, the adaptive region learning module contains learning of scaling factors to change the size of the corresponding muscle regions, as well as offset learning to slightly adjust landmark differences, with respect to different individuals. This suggests that adaptive region learning could better help the model to focus more accurately on the muscle region changes corresponding to each AU, and to obtain stronger robustness and generalisation ability. In addition, we did not evaluate the generalizability and transferability of the AU recognition presented in the previous version, whereas we attempt in the present study. Facial paralysis estimation is a time-consuming and subjective task for a traditional physician's diagnosis. Facial palsy is a condition characterised by motor dysfunction of the muscles of facial expression. It is usually qualified by observing the activation status of certain muscle areas and facial symmetry when the patient makes certain expressions, such as basic eyebrow raising, eye closing and mouth puckering, *etc.* In this study, we apply the proposed ALGRNet on facial paralysis estimation, which can improve the effectiveness of facial paralysis recognition and estimation by focusing on the activation of multiple muscle regions as well as global facial information. Specially, we collect a facial paralysis dataset which is annotated by medical professions to four grades of facial palsy degrees, *i.e.* normal, low, medium and high grade. For the facial paralysis estimation we focus on the muscle areas that are more preferred in the facial paralysis ratings rather than the AU predefined muscle regions. Finally, we combine the multiple muscle region features enhanced by the interaction, as well as the useful global information, to obtain the final facial features for the facial palsy grade classification. To the best of our knowledge, there is no existing work in the literature on the estimation of facial paralysis using AU recognition methods. And we shows the effectiveness and transferability of the proposed ALGRNet quantitatively through the Facial Palsy Assessment application, which was not present in our earlier conference version [18].

II. RELATED WORK

A. Facial Action Units Recognition

AU recognition has been studied for decades and several methods have been proposed for this problem. Most existing methods for AU recognition are based on patch learning [19]–[23]. For instance, [24] used sparse coding to recover facial expressions using the composition rules of different fixed patches for different AUs. [21] proposed to use domain knowledge and facial geometry to pre-select a relevant image region for a particular AU and feed it to a convolutional and bi-directional Long Short-Term Memory (LSTM) neural network. However, all above methods need to predefined the patch location first. To address these issues, [16] combined facial AU recognition and face alignment in an end-to-end framework, where the face alignment results can aid AUs to learn the irregular attention distribution of the ROI of AU patches. Recent works in facial AU recognition also pay attention to capture the interactions of different AUs for local feature enhancement with multi-label learning. On one hand, taking into account the relationship of multiple face patches

can provide more robustness than using single patch. [25] embedded the relations among AUs through a predefined graph convolutional network (GCN). [26] incorporated AU knowledge-graph as an extra guidance to enhance the facial region representation. However, these methods need the prior connections by co-occurrence probability in different datasets. On the other hand, some approaches tried to apply the local relationship information into multi-label learning. For instance, [13] proposed a joint patch learning and multi-label learning method, in which the local regions of AUs are defined as patches centered around the facial landmarks.

In contrast to previous studies, ALGRNet automatically models the relation structure of the facial AUs by the use of a contextual structure along with a skipping operation. The most relevant existing works to ours are [15], [16], which combine facial AU recognition and face alignment into a multiple independent branches network. Different from these methods, our ALGRNet is capable of exploiting the learned correspondence of different AUs to enhance the target local AU, as well as considering other non-AU regions. Doing so allows us to provide more robustness than [15], which also improves the interpretability of the model.

B. Facial Paralysis Estimation

Facial paralysis estimation has recently attracted extensive research attention [27], [28], due to the significant psychological and functional impairment to patients. Nottingham system [29] is a widely accepted system for the clinical assessment of facial nerve function, which is similar with House-Brackmann (H-B) [30]. In addition to these, there are over twenty other methods of recognising and assessing facial palsy that are available in the literature. However, all of the above traditional methods are estimated by medical professionals and are both time consuming and subjective. More Recently, deep learning has been widely applied for facial representation learning, including using the deep representation for face recognition, face alignment, *etc.* [31] and [32] proposed two efficient quantitative assessment of facial paralysis based on the detected key points. [33] proposed to obtain the facial paralysis degree by calculating the changes of the surface areas of specific facial region. [34] considered both static facial asymmetry and dynamic transformation factors to evaluate the degree of facial paralysis. However, most of the exiting methods were only used the deep learning methods to pave the way for physical computation and do not directly model and predict the depth features of a face image. In addition, they apply some post-processing to obtain the final result.

In contrast to these existing methods, we employ an end-to-end deep framework ALGRNet to predict the grade of facial paralysis. We perform an automated estimation by combining depth features from high interest muscle regions with feature information from the global face, without any post-processing.

III. APPROACH

Fig. 2 shows the overall diagram of the proposed ALGRNet approach, which consists of adaptive region learning module

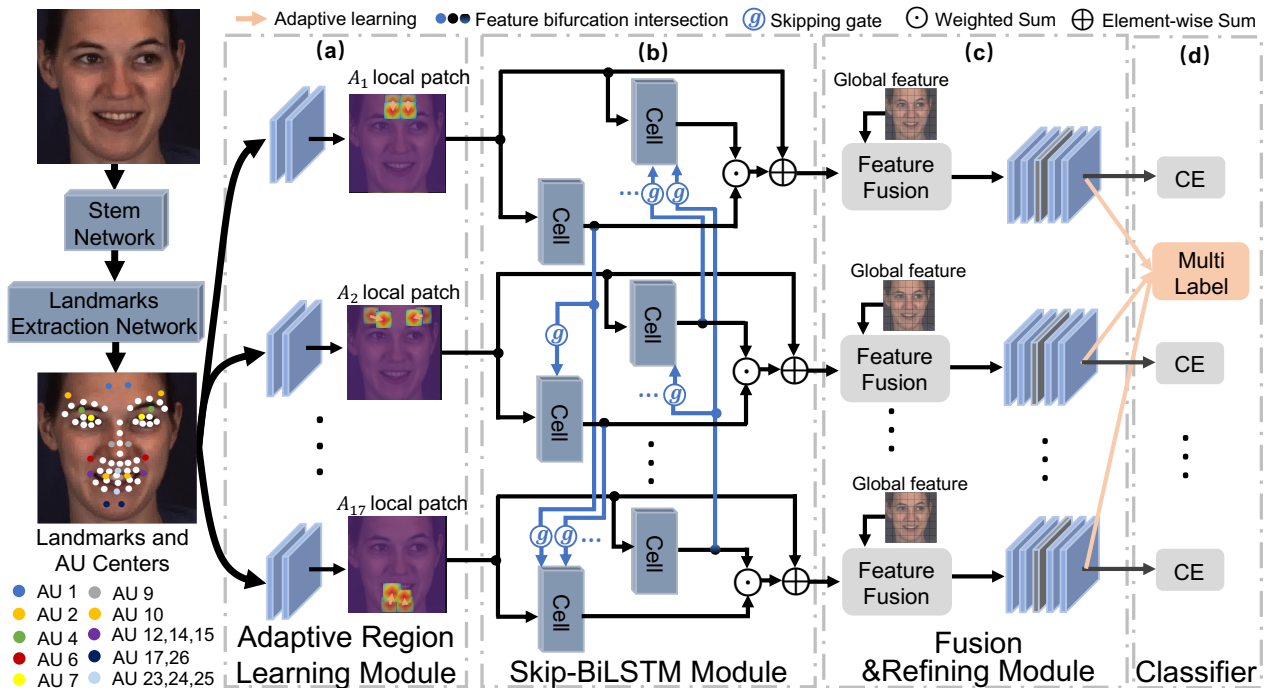


Fig. 2. The overall architecture of the proposed ALGRNet for facial AU recognition. We utilize a simple landmark localization network to detect the landmarks and two linear-based network to learn the offsets and scaling factor of AU centers, which are used to compute local AU patches. The AU patches are fed into our multi-branch network, with one branch per AU, and a skip-BiLSTM module is proposed to model mutual assistance and exclusion relationship among different AU branches. Then, a feature fusion&refining module is designed to refine the local features with the assistance of the global grid-based features; so that they can capture more discriminative features for AU with irregular shapes. Finally, a multi-classifier is used to predict the activation probabilities of individual AUs (best viewed in color).

for adaptive muscle region localisation, a skip-BiLSTM module for mutual assistance and exclusion modeling, a feature fusion&refining module for refining features of irregular AU regions, and a multi-classifier module for predicting the AU activation probability. We provide the details below.

A. Overview of ALGRNet

Similar to [15], [16], [35], we also employ a multi-branch network for the multi-label facial AU recognition task. However, different from previous approaches, we argue that exploiting the relationship among multiple patches plays a vital role in building a robust AU recognition model. In addition, due to the diversity of expressions and individual characteristics, we also attempted to learn adaptive muscle region offsets and scaling factors for each AU region. In this way, we design three modules (adaptive region learning module, skip-BiLSTM module and Fusion&Refining module) based on the foundation of existing multi-branch network, which can fully mine the local and global interactive relations among the AU patches based on the corresponding adaptive muscle regions and non-AU regions, and obtain a more discriminative and robust representation.

We first adapt a stem network from the widely used multi-branch network [16], which contains a hierarchical and multi-scale region learning network for the local muscle region feature and global feature extraction. However, unlike the predefined the muscle regions based on the detected landmark in [16], we add two simple network combined with

the previous face alignment network, named adaptive region learning module (detailed in Section III-B), to adaptively learn the offsets and scaling factors for each region. After that, local patches $A = \{A_1, A_2, \dots, A_n\}$ are calculated and their features $V = \{v_1, v_2, \dots, v_n\}$ are extracted via the stem network based on the learned location, where n is the numbers of selected patches, respectively. For simplicity, we do not repeat the detailed structure of the stem network here.

In order to overcome the lack of adequate delivery of local patch information among individual patches, we design a novel skip-BiLSTM module (detailed in Section III-C), which can transmit information in two ways (sequential delivery or skipping delivery). The sequential delivery of information can fully explore the contextual relationship between adjacent patches. The skipping delivery focuses on the information interactive of non-adjacent related patches. Different from the traditional sequence spreading of LSTM, our skip-BiLSTM can directly calculate the correlation between a target AU and all previous AUs in the forward and backward directions. This is beneficial because there is little information loss during multi-branch transmission. After skip-BiLSTM, we get a set of local patch features $S = \{s_1, s_2, \dots, s_n\}$, which are expected to have all the useful information from adjacent and non-adjacent patches.

Furthermore, we argue that the non-AU regions can be helpful for refining the local patch features and obtain salient micro-level features for the global face, which may be useful for handling irregular AU regions. Hence, we design a novel feature Fusion&Refining module (detailed in Section III-D),

which can concentrate on the salient information from global facial feature G . Finally, the local patch features are integrated with global facial features as new patch-based representation $R = \{r_1, r_2, \dots, r_n\}$.

The face alignment and facial AU recognition are integrated into an end-to-end learning model. Our goal is to jointly learn all the parameters by minimizing both face alignment loss and facial AU recognition loss over the training set. The face alignment loss is defined as:

$$\mathcal{L}_{align} = \frac{1}{2d_o^2} \sum_{i=1}^m [(x_i - \hat{x}_i)^2 + (y_i - \hat{y}_i)^2], \quad (1)$$

where (x_i, y_i) and (\hat{x}_i, \hat{y}_i) denote the ground-truth (GT) coordinate and corresponding predicted coordinate of the i -th facial landmark, and d_o is the ground-truth inter-ocular distance for normalization [15]. In this paper, we also regard facial AU recognition as a multi-label binary classification task following [15]. It can be formulated as a supervised classification training objective as follows,

$$\mathcal{L}_{rec} = -\frac{1}{n} \sum_{i=1}^n w_i [p_i \log \hat{p}_i + (1 - p_i) \log (1 - \hat{p}_i)], \quad (2)$$

where p_i denotes the GT probability of occurrence for the i -th AU, which is 1 if occurrence and 0 otherwise, and \hat{p}_i denotes the predicted probability of occurrence. w_i is the data balance weights, which is employed in [16]. Moreover, we also employ a weighted multi-label Dice coefficient loss [36] to overcome the sample imbalance problem, which is formulated as:

$$\mathcal{L}_{dice} = \frac{1}{n} \sum_{i=1}^n w_i \left(1 - \frac{2p_i \hat{p}_i + \tau}{p_i^2 \hat{p}_i^2 + \tau}\right), \quad (3)$$

where τ is the smoothness parameter. Finally, the facial AU recognition loss is defined as:

$$\mathcal{L}_{au} = \mathcal{L}_{rec} + \mathcal{L}_{dice}, \quad (4)$$

Furthermore, we also minimize the loss of AU category classification \mathcal{L}_{int} by integrating all AUs information, including the refined AU features and the face alignment features, which is similar to the processing of \mathcal{L}_{au} .

Finally, the joint loss of our ALGRNet is defined as:

$$\mathcal{L} = (\mathcal{L}_{au} + \mathcal{L}_{int}) + \lambda \mathcal{L}_{align}. \quad (5)$$

where λ is a balancing parameter.

B. Adaptive region learning module

Instead of predefined the muscle region directly from the detected landmarks, we use two simple fully connected networks to adaptively learn the offsets and scaling factors for all AU regions respectively. Specially, we utilize an efficient landmark extraction network after the stem network to extract the landmarks $L = \{l_1, l_2, \dots, l_m\}$ (m is the numbers of landmarks) similar to [15], including three convolutional layers connected to a max-pooling layer. Simultaneously, two networks containing two fully-connected layers are used to get the adaptive offsets $O = \{o_1, o_2, \dots, o_{2n}\}$ and scaling factors $E = \{e_1, e_2, \dots, e_n\}$ respectively. According to the

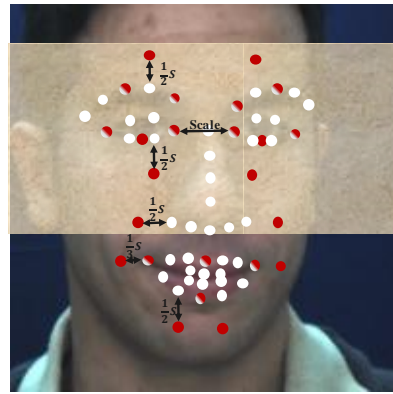


Fig. 3. New definitions for the 12 locations of muscle centers of facial paralysis estimation, which are marked in red or mixed red. The detected landmarks are marked in white or mixed red. “Scale” denotes the distance between two inner eye corners.

learned landmarks, offsets and scaling factors, local patches A are calculated. In particular, we first use the same rules in [15] to get the locations of AU centers based on the detected landmarks and then update the by adding the learned offsets. Please note that, we change the predefined muscle region centers, as shown in Fig. 3¹, based on the detected landmarks when we apply ALGRNet on facial paralysis estimation. Different from [15], we make the scaling factor E learnable rather than a fixed value, where e_i is the width ratio between the region of AU_i and whole feature map. After that, we generate an approximate Gaussian attention distribution for each AU region following [16]. Finally, based on the learned regions, local patch features V are extracted via the stem network.

C. Skip-BiLSTM

Fig. 2 (b) shows the detailed structure of our skip-BiLSTM module for contextual and skipping relationship learning. Specifically, we extract a set of local patch features $V = \{v_1, v_2, \dots, v_n\}$ from the stem network, and feed them to skip-BiLSTM. Distinct from the prior works [11], we regard the multiple patches as a sequence structure from top to bottom, which can transfer information by a Bi-directional LSTM based model [17] with our skipping-type gate. Different from the traditional BiLSTM or tree-LSTM [37], [38], our skip-BiLSTM can directly calculate the correlation between a target AU and all other AUs. For the t -th patch ($t > 1$), the extracted feature v_t is used to learn the weights with forward hidden states $H = \{h_1, \dots, h_{t-1}\}$ by the skipping-type gates, which can determine the correlation coefficient between past AUs and current AU. And then the new states $\hat{H} = \{\hat{h}_1, \dots, \hat{h}_{t-1}\}$ and v_t are fed into the t -th forward cell in the skip-BiLSTM to learn the association weights, which can promote the transfer of relevant AUs information. The above process can be formulated as:

$$\vec{h}_t = \text{Cell} \left(\sum_{j=1}^{t-1} \vec{h}_j, v_t \right), \quad (6)$$

¹Due to patient confidentiality agreements, we cannot show real patients with facial palsy. This example image is from BP4D.

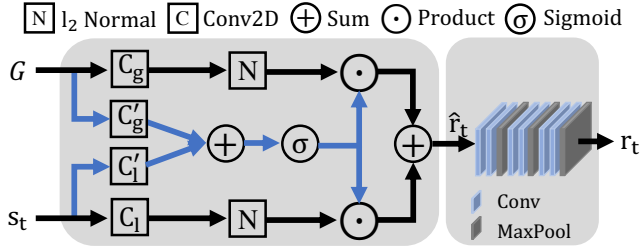


Fig. 4. The architecture of our feature fusion&refining module guided by global face feature.

$$\vec{h}_j = \vec{h}_j f_j, \quad (7)$$

$$f_j = \sigma(\text{GAP}(W_j(\vec{h}_j v_t))), \quad (8)$$

where $\text{Cell}(\cdot)$ denotes the basic ConvLstm cell [39], σ is sigmoid function, and GAP denotes the global average pooling operation. W_j is the parameters of mapping function, in which we used Conv2D. For the backward delivery, we get the t -th patch feature which goes to the same forward process as:

$$\overleftarrow{h}_t = \text{Cell}\left(\sum_{j=t+1}^n \overleftarrow{h}_j, v_t\right), \quad (9)$$

In order to fully promote the information interactive among individual AUs, the final representation for each patch is computed as the average of the hidden vectors in both directions, as well as the original patch feature:

$$s_t = v_t + (\vec{h}_t + \overleftarrow{h}_t)/2, \quad (10)$$

D. Feature Fusion&Refining

To exploit the useful global face feature, we design a gated fusion architecture and a refining architecture (F&R) that can selectively balance the relative importance of local patches and global face grids. We add these two architectures on each local AU branch because different AUs may focus on different global information. The grid-based global face feature G is extracted using a simple CNN with the same structure as the face alignment network [15]. As shown in Fig. 4, after obtaining the learned t -th local patch feature, it is fused with the grid-based global feature G by the fusion architecture, which can be formulated as:

$$\alpha = \sigma(C'_g G + C'_l s_t), \quad (11)$$

$$\hat{r}_t = \alpha \odot \|C_g G\|_2 \oplus (1 - \alpha) \odot \|C_l s_t\|_2, \quad (12)$$

where σ is the sigmoid function, and $\|\cdot\|$ denotes the l_2 -normalization. C'_* and C_* denote the Conv2D operation. \oplus denotes the element-wise weighted sum of $\|C_g G\|_2$ and $\|C_l s_t\|_2$ according to the learned gate vector α .

The final local fusion feature s_t for t -th patch refined by our F&R module is shown in Fig. 4. F&R module contains three blocks. Each block consists of two convolutional layers and a maxpooling layer. Then multi-patch features R are sent to the multi-label binary classifier to calculate the occurrence probabilities of individual AUs.

TABLE I

OVERVIEW INFORMATION OF OUR COLLECTED FACIAL PARALYSIS DATASET.

Grade	Normal	Low	Medium	High
Num. of Video	20	29	20	20
Num. of Frame	9049	16970	11019	10547

IV. EXPERIMENTS

A. Dataset and Implementation Detail

Dataset. We evaluate the effectiveness of the proposed approach for facial AU recognition on the popular BP4D [40] and DISFA [41] datasets. **BP4D** consists of 328 facial videos from 41 participants (23 females and 18 males) who were involved in 8 sessions. Similar to [14], [15], [22], we consider 12 AUs and 140K valid frames with labels. **DISFA** consists of 27 participants (12 females and 15 males). Each participant has a video of 4, 845 frames. We also limited the number of AUs to 8 similar to [15], [22]. In comparison to BP4D, the experimental protocol and lighting conditions deliver DISFA to be a more challenging dataset. Following the experiment setting of [15], we evaluated the model using the 3-fold subject-exclusive cross-validation protocol.

In addition, we collected a facial paralysis dataset from NHS, named **FPara**, which consists of 89 videos of facial palsy patients performing various types of facial palsy exercises inline with the House-Brackmann (H-B) scale [30]. Each of the videos consisted of facial palsy patients performing the following exercises, such as raise eyebrows, close eyes gently, close eyes tightly, scrunch up face and smile, *etc.* They were part of a previous study on facial palsy with patient consent for research [42]. These videos are assigned a H-B scale from 1 to 6, and 1 being normal and 6 being severest with no body movements. We then further split into four grades, such as normal (H-B score=1), low (H-B score=2), medium ($3 \leq \text{H-B score} \leq 4$) and high ($5 \leq \text{H-B score} \leq 6$) grades. Similar to the settings of facial AU dataset, all facial paralysis grades are evaluated using subject exclusive 3-fold cross-validation, where two folds (about 80%) are used for training and the remaining one is used for testing (about 20%).

Training strategy. Our model is trained on a single NVIDIA Tesla V100 GPU with 32 GB memory. The whole network is trained using PyTorch [44] with the stochastic gradient descent (SGD) solver, a Nesterov momentum [45] of 0.9 and a weight decay of 0.0005. The learning rate is set to 0.01 initially with a decay rate of 0.5 every 2 epochs. Maximum epoch number is set to 20. To enhance the diversity of training data, aligned faces are further randomly cropped into 176×176 and horizontally flipped. Regarding face alignment network and stem network, we set the value of the general parameters to be the same with [15]. The filters for the convolutional layers in refining architecture are used 3×3 convolutional filters with a stride 1 and a padding 1. In our paper, all of the mapping Conv2D operations are used 1×1 convolutional filters with a stride 1 and a padding 1. The dimensionality of hidden state in ConvLstm cell is set to 64 and the filters for the convolutional layers in ConvLstm cell are used 3×3 convolutional filters

TABLE II
COMPARISONS OF AU RECOGNITION FOR 12 AUs ON BP4D IN TERMS OF F1-FRAME SCORE (IN %).

Method	AU Index												Avg.
	1	2	4	6	7	10	12	14	15	17	23	24	
EAC-Net [43]	39.0	35.2	48.6	76.1	72.9	81.9	86.2	58.8	37.5	59.1	35.9	35.8	55.9
MLCR [25]	42.4	36.9	48.1	77.5	77.6	83.6	85.8	61.0	43.7	63.2	42.1	55.6	59.8
JAA-Net [16]	47.2	44.0	54.9	77.5	74.6	<u>84.0</u>	86.9	61.9	43.6	60.3	42.7	41.9	60.0
LP-Net [11]	46.9	45.3	55.6	77.1	76.7	83.8	87.2	63.3	45.3	60.5	48.1	<u>54.2</u>	61.0
ARL [14]	45.8	39.8	55.1	75.7	<u>77.2</u>	82.3	86.6	58.8	<u>47.6</u>	62.1	47.4	55.4	61.1
J \hat{A} A-Net [15]	53.8	47.8	58.2	78.5	75.8	82.7	<u>88.2</u>	<u>63.7</u>	43.3	61.8	45.6	49.9	<u>62.4</u>
ALGRNet (Ours)	<u>51.2</u>	<u>48.2</u>	<u>57.3</u>	<u>77.9</u>	76.4	84.9	88.2	64.8	50.8	<u>62.8</u>	<u>47.6</u>	51.9	63.5

TABLE III
COMPARISONS OF AU RECOGNITION FOR 8 AUs ON DISFA IN TERMS OF F1-FRAME SCORE (IN %).

Method	AU Index								Avg.
	1	2	4	6	9	12	25	26	
EAC-Net [43]	41.5	26.4	66.4	50.7	80.5	89.3	88.9	15.6	57.4
JAA-Net [16]	43.7	46.2	56.0	41.4	44.7	69.6	88.3	58.4	56.0
LP-Net [11]	29.9	24.7	<u>72.7</u>	<u>46.8</u>	49.6	72.9	93.8	65.0	56.9
ARL [14]	43.9	42.1	63.6	41.8	40.0	<u>76.2</u>	95.2	66.8	58.7
J \hat{A} A-Net [15]	<u>62.4</u>	<u>60.7</u>	67.1	41.1	45.1	73.5	90.9	<u>67.4</u>	<u>63.5</u>
ALGRNet	63.8	65.4	73.6	44.5	<u>54.1</u>	74.0	<u>94.7</u>	69.9	67.5

TABLE IV
COMPARISONS OF FACIAL PARALYSIS ESTIMATION FOR 4 GRADES ON OUR NEW COLLECTED DATA, FPARA, IN TERMS OF F1-FRAME SCORE (IN %).

Method	Facial Paralysis Grades				Avg.
	Normal	Low	Medium	High	
ResNet18 [50]	99.8	50.7	47.7	67.9	66.5
ResNet50 [50]	99.9	53.9	54.7	71.4	70.0
Transformer-based [51]	100	63.0	58.6	68.7	72.6
J \hat{A} A-Net [15]	<u>100</u>	<u>58.8</u>	<u>64.3</u>	<u>72.9</u>	<u>72.8</u>
ALGRNet(Ours)	100	55.9	72.1	73.2	75.4

with a stride 1 and a padding 1. λ is set to 0.5 for the jointly optimizing of face alignment and facial AU recognition. For comparison purpose, the numbers of AUs are 12 (as in [14], [15], [22]) and 8 (as in [15], [22]) for BP4D and DISFA respectively. During training, each frame is annotated with 49 landmarks detected and calculated by SDM [46]. Different from J \hat{A} A-Net [15], we averaged the predicted probability of the local information and the integrated information as the final predicted activation probability for each AU, rather than simply using the integrated information of all the AUs.

Performance Metric. We evaluate the performance of all methods in terms of the F1 score (%) which has been widely used for classification. F1-frame score is the harmonic mean of the Precision P and Recall R and calculated by $F1 = 2PR/(P + R)$. For all methods, F1 score for all the AUs on BP4D and DISFA and for all facial paralysis grades on facial paralysis dataset are calculated and then averaged (denoted as **Avg.**) separately for comparison with “%” omitted.

B. Comparison with State-of-the-art Methods

1) *Facial Action Units Recognition:* We compare our proposed ALGRNet with several baselines on the BP4D and DSIFA datasets in Table II and Table III, including EAC-Net [43], MLCR [25], JAANet [16], LP-Net [11], ARL [14], and J \hat{A} A-Net [15]. Note that, the best and second best results are shown using bold and underline, respectively. The performances of the baselines in Table III and II are the reported

results. We omit models [47]–[49] that require additional annotated data.

Quantitative comparison on BP4D: AU recognition results by different methods on BP4D are shown in Table II, where the proposed ALGRNet outperforms the state-of-the-art methods with impressive margins. ALGRNet achieves 1.1% higher average F1 score compared with J \hat{A} A-Net. Furthermore, ALGRNet achieves the best or second-best recognition performance for most of the 12 AUs annotated in BP4D compared with the state-of-the-art methods.

Quantitative comparison on DISFA: AU recognition results by different methods on DISFA are shown in Table III, where the proposed ALGRNet shows clear improvements for several AUs annotated in DISFA compared with the state-of-the-art methods. Specifically, compared with the state-of-the-art method J \hat{A} A-Net [15], our ALGRNet achieves 4.0% improvements in terms of average F1 score and also achieves significantly outperforms for all AUs annotated in DISFA. Furthermore, we achieve the best performance in terms of average F1 score compared with all baselines.

2) *Facial Paralysis Estimation:* Different with facial AU recognition, the exiting deep-learning-based facial paralysis estimation methods are rare, so we apply currently popular deep learning classification methods, such as the ResNet [50] and Transformer [52], on our collected facial palsy dataset (FPara). Besides, we also compare it with the state-of-the-art AU recognition approach, J \hat{A} A-Net [15]. Specially, we evaluate the following methods:

TABLE V

EFFECTIVENESS OF KEY COMPONENTS OF LGRNET EVALUATED ON DISFA IN TERMS OF F1-FRAME SCORE (IN %).

Methods	Setting			AU Index								Avg.
	S-B	F&R	Ada	1	2	4	6	9	12	25	26	
w/o full				47.1	61.1	66.3	<u>44.7</u>	52.2	74.9	92.2	66.2	63.1
w/o F&R	✓			62.6	64.2	72.4	42.3	49.9	76.1	93.5	<u>72.6</u>	<u>66.7</u>
w/o S-B		✓		58.7	<u>65.2</u>	<u>73.5</u>	43.9	<u>53.5</u>	72.2	94.1	64.7	65.7
w/ Bi		✓		61.1	58.4	70.9	45.5	47.9	74.9	92.5	70.8	65.2
w/o Ada	✓	✓		<u>62.6</u>	64.4	72.5	46.6	48.8	<u>75.7</u>	<u>94.4</u>	73.0	67.3
ALGRNet	✓	✓	✓	63.8	65.4	73.6	44.5	54.1	74.0	94.7	69.9	67.5

TABLE VI

EFFECTIVENESS OF KEY COMPONENTS OF LGRNET EVALUATED ON BP4D IN TERMS OF F1-FRAME SCORE (IN %).

Methods	Setting			AU Index												Avg.
	S-B	F&R	Ada	1	2	4	6	7	10	12	14	15	17	23	24	
w/o full				50.1	47.1	54.3	77.3	75.1	82.5	88.1	61.7	44.9	62.7	45.2	49.9	61.6
w/o F&R	✓			50.4	46.9	53.4	79.0	<u>77.4</u>	<u>84.7</u>	87.4	63.0	45.3	63.3	47.0	55.7	62.8
w/o S-B		✓		51.3	47.6	56.3	<u>78.2</u>	76.2	83.7	88.1	64.4	49.1	61.9	46.1	49.8	62.7
w/ Bi		✓		50.7	50.0	55.2	77.0	75.7	84.1	<u>88.2</u>	63.4	49.1	62.3	<u>47.3</u>	52.0	62.9
w/o Ada	✓	✓		50.8	47.1	57.8	77.6	77.4	<u>84.7</u>	88.2	66.4	<u>49.8</u>	61.5	46.8	<u>52.3</u>	<u>63.4</u>
ALGRNet	✓	✓	✓	<u>51.2</u>	<u>48.2</u>	<u>57.3</u>	77.9	76.4	84.9	88.2	<u>64.8</u>	50.8	<u>62.8</u>	47.6	51.9	63.5

- ResNet18 and ResNet50 [50]: These methods use different depth layers based on ResNet to model the input face images, which are similar to [53].
- Transformer-based method [51]: This baseline is motivated from self-attention and uses the Transformer [52] architecture. The output of the Transformer-based encoder [51] is treated as the latent representation for the input of the multi-label AU classifier.
- JAA-Net [15]: This is a recently proposed multi-branch combination-based AU recognition method, which can extract precise local muscle features thanks to a joint facial alignment network.

Quantitative comparison on the collected FPara: Facial paralysis estimation results by different methods on our FPara are shown in Table IV. It has been shown that our ALGRNet outperforms all its competitors with impressive margins. Specifically, compared with the state-of-the-art AU recognition method JAA-Net [15], our ALGRNet achieves 2.6% improvements in terms of average F1 score. Moreover, the average F1 score of our ALGRNet get 2.8% higher compared to the currently popular Transformer-based approach [51].

Experimental results of our ALGRNet demonstrate its effectiveness in improving AU recognition accuracy on BP4D and DISFA, as well as good generalization ability on our new facial paralysis dataset.

C. Ablation Studies

We perform detailed ablation studies on DISFA and BP4D to investigate the effectiveness of each component of our

proposed ALGRNet for facial AU recognition.

1) *Effects of adaptive region learning module:* To cancel out the adaptive region learning (indicated w/o Ada), we follow the same experiment setting as [15] (It means each scaling factor e is set to 0.14.) to predefined muscle region based on the detected landmarks for each AU. In Table V and VI, ALGRNet decreases its F1 score to 67.3% and 63.4% on DISFA and BP4D respectively. It has been shown that the adaptive region learning module can contribute the AU recognition greatly.

2) *Effects of skip-BiLSTM:* In Table V and VI, ALGRNet (without adaptive region learning module) decreases absolutely by 1.6% and 0.7% in terms of average F1 score when removing skip-BiLSTM (indicated by w/o S-B) on DISFA and BP4D, respectively. Furthermore, in order to fully verify the effectiveness of our skipping operation, we replace skip-BiLSTM with the basic BiLSTM [17] (indicated by w/ Bi) for information delivery between multiple branches in our ALGRNet (also with Fusion&Refining module), ALGRNet achieves lower average F1 scores of 65.2% and 62.9% on DISFA and BP4D, respectively. These observations indicate that a rough definition of the relationship between AUs from top to bottom may not be the best way to simulate the real relationship between AUs. And skipping operation can significantly boost the performance, which suggests that our skipping-type gates play a vital role in our model. In addition, these results also indicate that using skip-BiLSTM to model the mutual assistance and exclusion relationship between AUs is effective for improve AU recognition accuracy.

3) *Effects of feature fusion&refining module:* Without fusion&refining module (indicated by w/o F&R in Table V and

TABLE VII

MEAN ERROR (%) RESULTS OF DIFFERENT FACE ALIGNMENT MODELS ON DISFA AND BP4D (LOWER IS BETTER).

Methods	DISFA	BP4D	FPara
J \hat{A} A-Net	3.87	3.80	5.15
ALGRNet	3.29	3.78	5.18

VI), we directly conduct classification over the output of skip-BiLSTM. Great AU recognition performance degradation can be observed, *i.e.*, 0.6% average F1 score drop on DISFA and BP4D. It suggests that the proposed fusion&refining module, which refines local AU feature guided by grid-based global feature, plays a vital role in our model.

Finally, when we simultaneously drop the adaptive region learning module, skip-BiLSTM and fusion&refining modules (indicated by w/o full in Table V and VI), the average F1 score of our method reduces from 67.5% to 63.1% on DISFA, and from 63.5% to 61.6% on BP4D, respectively. We have observed that considering the adaptive region learning, skip-BiLSTM and fusion&refining modules together can significantly boost the performance of facial AU recognition.

D. Results for Face Alignment

We jointly take face alignment network into our ALGRNet via auxiliary training, which can provide effective muscle regions based on the detected landmarks corresponding to each AU. Table VII shows the mean error results of our ALGRNet and baseline method J \hat{A} A-Net [15] on DISFA, BP4D and FPara. Compared with J \hat{A} A-Net, our ALGRNet achieves competitive 3.29, 3.78 and 5.18 mean error on DISFA, BP4D and FPara respectively, which indicates the effectiveness of our joint training. The robustness of the adaptive region learning module allows our ALGRNet to outperform J \hat{A} A-Net in AU recognition and facial paralysis estimation, even if sometimes with slightly lower landmark detection accuracy.

E. Visualization of Results

To better understand the effectiveness of our proposed model, we visualize the learned class activation maps of ALGRNet (the outputs of F&R module), corresponding to different AUs, as shown in Fig. 5. Four examples from two different datasets are given, two of which are from BP4D and two are from DISFA, containing visualization results of different genders with different AU categories. Through the learning of ALGRNet, local patches not only concentrate on their own regions, but can also establish a positive correlation with other patches as well as other non-AU regions. Different from the excessive localization of J \hat{A} A-Net [15] and the bad influence of unrelated regions of ARL [16], our ALGRNet accurately captures potential mutual assistance (in red) and mutual exclusion (in blue) relationships of the local patch feature for each AU and other assistance AUs, as well as non-AU regions in global face, which can improve the discriminative ability of each AU. The heatmaps of the same AU category in different examples are roughly consistent, but there

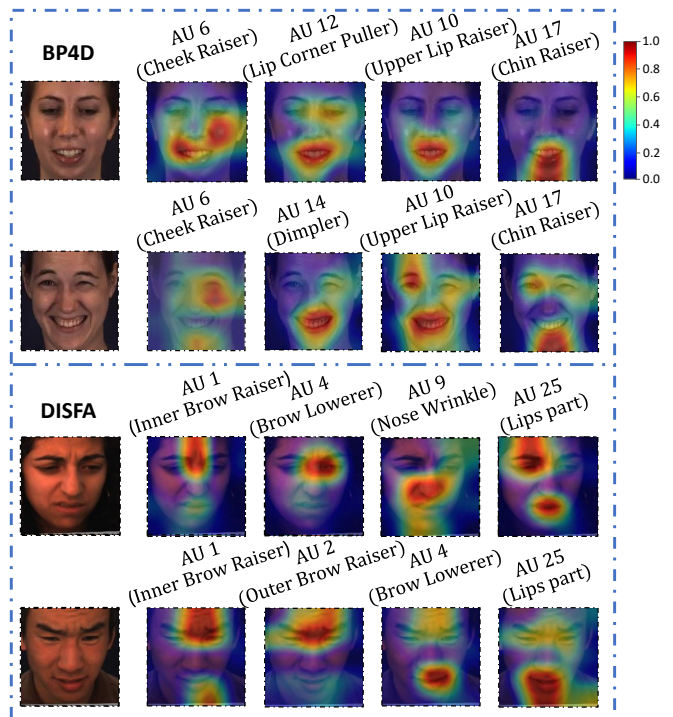


Fig. 5. Class activation maps that show the discriminative regions for different AUs in terms of different expressions and individuals on DISFA and BP4D datasets.

are also differences due to individual differences. This reveals that our ALGRNet can learn certain rules in different datasets and adaptively make adjustments based on different samples, compared with the predefined GCN methods [25], [26].

V. CONCLUSION

In this work, we study the problem of facial action units recognition and facial paralysis estimation. We propose a novel multi-branch multi-label based approach namely ALGRNet. The proposed approach adaptively catches the corresponding muscle areas in terms of different expressions and individuals. Then it enables efficient information delivery via a novel skip-BiLSTM and models the potential mutual assistance and exclusion relationships among the branches for local AU features. ALGRNet also consists of a feature fusion&refining module that exploits complementarity between local feature and grid-based global feature to obtain refined local region features. Extensive experimental evaluations on two widely used AU recognition benchmarks and a new collected facial paralysis estimation benchmark show that our ALGRNet is able to learn more robustness and discriminative features for facial AU recognition and migrates well to the facial paralysis estimation task.

REFERENCES

- [1] D. R. Rubinow and R. M. Post, "Impaired recognition of affect in facial expression in depressed patients," *Biological psychiatry*, vol. 31, no. 9, pp. 947–953, 1992.
- [2] X. Niu, H. Han, J. Zeng, X. Sun, S. Shan, Y. Huang, S. Yang, and X. Chen, "Automatic engagement prediction with gap feature," in *ICMI*, 2018, pp. 599–603.

- [3] R. S. Feldman, L. Jenkins, and O. Popoola, "Detection of deception in adults and children via facial expressions," *Child development*, pp. 350–355, 1979.
- [4] B. Klare and A. K. Jain, "Heterogeneous face recognition: Matching nir to visible light images," in *ICPR*, 2010, pp. 1513–1516.
- [5] M. N. Butt and M. Iqbal, "Teachers' perception regarding facial expressions as an effective teaching tool," *Contemporary Issues in Education Research*, vol. 4, no. 2, pp. 11–14, 2011.
- [6] P. Ekman and E. L. Rosenberg, *What the face reveals: Basic and applied studies of spontaneous expression using the Facial Action Coding System (FACS)*. Oxford University Press, USA, 1997.
- [7] Y. Tong and Q. Ji, "Learning bayesian networks with qualitative constraints," in *CVPR*, 2008, pp. 1–8.
- [8] Y. Li, S. Wang, Y. Zhao, and Q. Ji, "Simultaneous facial feature tracking and facial expression recognition," *IEEE Trans. Image Process.*, vol. 22, no. 7, pp. 2559–2573, 2013.
- [9] P. Liu, S. Han, Z. Meng, and Y. Tong, "Facial expression recognition via a boosted deep belief network," in *CVPR*, 2014, pp. 1805–1812.
- [10] P. Liu, J. T. Zhou, I. W.-H. Tsang, Z. Meng, S. Han, and Y. Tong, "Feature disentangling machine—a novel approach of feature selection and disentangling in facial expression analysis," in *ECCV*, 2014, pp. 151–166.
- [11] X. Niu, H. Han, S. Yang, Y. Huang, and S. Shan, "Local relationship learning with person-specific shape regularization for facial action unit detection," in *CVPR*, 2019, pp. 11917–11926.
- [12] S. Hochreiter and J. Schmidhuber, "Long short-term memory," *Neural Computation*, vol. 9, no. 8, pp. 1735–1780, 1997.
- [13] K. Zhao, W.-S. Chu, F. De la Torre, J. F. Cohn, and H. Zhang, "Joint patch and multi-label learning for facial action unit and holistic expression recognition," *IEEE Trans. Image Process.*, vol. 25, no. 8, pp. 3931–3946, 2016.
- [14] Z. Shao, Z. Liu, J. Cai, Y. Wu, and L. Ma, "Facial action unit detection using attention and relation learning," *IEEE Trans. Affective Comput.*, 2019.
- [15] Z. Shao, Z. Liu, J. Cai, and L. Ma, "Jaa-net: joint facial action unit detection and face alignment via adaptive attention," *IJCV*, vol. 129, no. 2, pp. 321–340, 2021.
- [16] —, "Deep adaptive attention for joint facial action unit detection and face alignment," in *ECCV*, 2018, pp. 705–720.
- [17] A. Graves and J. Schmidhuber, "Framewise phoneme classification with bidirectional lstm and other neural network architectures," *Neural Networks*, vol. 18, no. 5–6, pp. 602–610, 2005.
- [18] X. Ge, P. Wan, H. Han, J. M. Jose, Z. Ji, Z. Wu, and X. Liu, "Local global relational network for facial action units recognition," in *FG*. IEEE, 2021, pp. 01–08.
- [19] L. Zhong, Q. Liu, P. Yang, J. Huang, and D. N. Metaxas, "Learning multiscale active facial patches for expression analysis," *IEEE Trans. Cybern.*, vol. 45, no. 8, pp. 1499–1510, 2014.
- [20] K. Zhao, W.-S. Chu, F. De la Torre, J. F. Cohn, and H. Zhang, "Joint patch and multi-label learning for facial action unit detection," in *CVPR*, 2015, pp. 2207–2216.
- [21] S. Jaiswal and M. Valstar, "Deep learning the dynamic appearance and shape of facial action units," in *WACV*, 2016, pp. 1–8.
- [22] W. Li, F. Abtahi, and Z. Zhu, "Action unit detection with region adaptation, multi-labeling learning and optimal temporal fusing," in *CVPR*, 2017, pp. 1841–1850.
- [23] C. Ma, L. Chen, and J. Yong, "Au r-cnn: Encoding expert prior knowledge into r-cnn for action unit detection," *Neurocomputing*, vol. 355, pp. 35–47, 2019.
- [24] S. Taheri, Q. Qiu, and R. Chellappa, "Structure-preserving sparse decomposition for facial expression analysis," *IEEE Trans. Image Process.*, vol. 23, no. 8, pp. 3590–3603, 2014.
- [25] X. Niu, H. Han, S. Shan, and X. Chen, "Multi-label co-regularization for semi-supervised facial action unit recognition," in *NeurIPS*, 2019, pp. 909–919.
- [26] G. Li, X. Zhu, Y. Zeng, Q. Wang, and L. Lin, "Semantic relationships guided representation learning for facial action unit recognition," in *AAAI*, vol. 33, 2019, pp. 8594–8601.
- [27] M. J. Fields and N. S. Peckitt, "Facial nerve function index: a clinical measurement of facial nerve activity in patients with facial nerve palsies," *Oral surgery, oral medicine, oral pathology*, vol. 69, no. 6, pp. 681–682, 1990.
- [28] E. A. Chu, T. Y. Farrag, L. E. Ishii, and P. J. Byrne, "Threshold of visual perception of facial asymmetry in a facial paralysis model," *JAMA Facial Plast. Surg.*, vol. 13, no. 1, pp. 14–19, 2011.
- [29] G. E. Murty, J. P. Diver, P. J. Kelly, G. O'Donoghue, and P. J. Bradley, "The nottingham system: objective assessment of facial nerve function in the clinic," *Otolaryngology—Head and Neck Surgery*, vol. 110, no. 2, pp. 156–161, 1994.
- [30] W. House, "Facial nerve grading system," *Otolaryngol Head Neck Surg*, vol. 93, pp. 184–193, 1985.
- [31] J. Dong, L. Ma, Q. Li, S. Wang, L.-a. Liu, Y. Lin, and M. Jian, "An approach for quantitative evaluation of the degree of facial paralysis based on salient point detection," in *IITA*. IEEE, 2008, pp. 483–486.
- [32] J. Barbosa, K. Lee, S. Lee, B. Lodhi, J.-G. Cho, W.-K. Seo, and J. Kang, "Efficient quantitative assessment of facial paralysis using iris segmentation and active contour-based key points detection with hybrid classifier," *BMC medical imaging*, vol. 16, no. 1, pp. 1–18, 2016.
- [33] G. Cheng, J. Dong, S. Wang, H. Qu *et al.*, "Evaluation of facial paralysis degree based on regions," in *KDD*. IEEE, 2010, pp. 514–517.
- [34] T. Wang, S. Zhang, J. Dong, L. Liu, and H. Yu, "Automatic evaluation of the degree of facial nerve paralysis," *Multimed. Tools. Appl.*, vol. 75, no. 19, pp. 11893–11908, 2016.
- [35] C. Corneanu, M. Madadi, and S. Escalera, "Deep structure inference network for facial action unit recognition," in *ECCV*, 2018, pp. 298–313.
- [36] F. Milletari, N. Navab, and S.-A. Ahmadi, "V-net: Fully convolutional neural networks for volumetric medical image segmentation," in *3DV*, 2016, pp. 565–571.
- [37] K. S. Tai, R. Socher, and C. D. Manning, "Improved semantic representations from tree-structured long short-term memory networks," in *ACL*, 2015, pp. 1556–1566.
- [38] X. Ge, F. Chen, J. M. Jose, Z. Ji, Z. Wu, and X. Liu, "Structured multi-modal feature embedding and alignment for image-sentence retrieval," in *ACM MM*, 2021, pp. 5185–5193.
- [39] X. Shi, Z. Chen, H. Wang, D.-Y. Yeung, W.-K. Wong, and W.-c. Woo, "Convolutional lstm network: A machine learning approach for precipitation nowcasting," *NeurIPS*, pp. 802–810, 2015.
- [40] X. Zhang, L. Yin, J. F. Cohn, S. Canavan, M. Reale, A. Horowitz, P. Liu, and J. M. Girard, "Bp4d-spontaneous: a high-resolution spontaneous 3d dynamic facial expression database," *Image and Vision Computing*, vol. 32, no. 10, pp. 692–706, 2014.
- [41] S. M. Mavadati, M. H. Mahoor, K. Bartlett, P. Trinh, and J. F. Cohn, "Disfa: A spontaneous facial action intensity database," *IEEE Trans. Affective Comput.*, vol. 4, no. 2, pp. 151–160, 2013.
- [42] B. F. O'Reilly, J. J. Soraghan, S. McGrenary, and S. He, "Objective method of assessing and presenting the house-brackmann and regional grades of facial palsy by production of a facogram," *Otology & Neurotology*, vol. 31, no. 3, pp. 486–491, 2010.
- [43] W. Li, F. Abtahi, Z. Zhu, and L. Yin, "Eac-net: Deep nets with enhancing and cropping for facial action unit detection," *IEEE Trans. Pattern Anal. Mach. Intell.*, vol. 40, no. 11, pp. 2583–2596, 2018.
- [44] A. Paszke, S. Gross, F. Massa, A. Lerer, J. Bradbury, G. Chanan, T. Killeen, Z. Lin, N. Gimelshein, L. Antiga *et al.*, "Pytorch: An imperative style, high-performance deep learning library," in *NeurIPS*, 2019, pp. 8026–8037.
- [45] I. Sutskever, J. Martens, G. Dahl, and G. Hinton, "On the importance of initialization and momentum in deep learning," in *ICML*, 2013, pp. 1139–1147.
- [46] X. Xiong and F. De la Torre, "Supervised descent method and its applications to face alignment," in *CVPR*, 2013, pp. 532–539.
- [47] N. N. Lakshminarayana, N. Sankaran, S. Setlur, and V. Govindaraju, "Multimodal deep feature aggregation for facial action unit recognition using visible images and physiological signals," in *FG*, 2019, pp. 1–4.
- [48] H. Yang, T. Wang, and L. Yin, "Adaptive multimodal fusion for facial action units recognition," in *Proceedings of the 28th ACM International Conference on Multimedia*, 2020, pp. 2982–2990.
- [49] P. Liu, Z. Zhang, H. Yang, and L. Yin, "Multi-modality empowered network for facial action unit detection," in *WACV*, 2019, pp. 2175–2184.
- [50] K. He, X. Zhang, S. Ren, and J. Sun, "Deep residual learning for image recognition," in *CVPR*, 2016, pp. 770–778.
- [51] J. M. J. Valanarasu, P. Oza, I. Hacıhaliloğlu, and V. M. Patel, "Medical transformer: Gated axial-attention for medical image segmentation," in *MICCAI*. Springer, 2021, pp. 36–46.
- [52] A. Vaswani, N. Shazeer, N. Parmar, J. Uszkoreit, L. Jones, A. N. Gomez, Ł. Kaiser, and I. Polosukhin, "Attention is all you need," *NeurIPS*, vol. 30, 2017.
- [53] A. Song, Z. Wu, X. Ding, Q. Hu, and X. Di, "Neurologist standard classification of facial nerve paralysis with deep neural networks," *Future Internet*, vol. 10, no. 11, p. 111, 2018.